PHYSICAL REVIEW A **94**, 053859 (2016)

Electromagnetically induced transparency and quantum heat engines

S. E. Harris*

Department of Electrical Engineering and Department of Applied Physics, Ginzton Laboratory, Stanford University, Stanford, California 94305, USA

(Received 28 June 2016; published 30 November 2016)

We describe how electromagnetically induced transparency may be used to construct a nontraditional near-ideal quantum heat engine as constrained by the second law. The engine is pumped by a thermal reservoir that may be either hotter or colder than that of an exhaust reservoir, and also by a monochromatic laser. As output, it produces a bright narrow emission at line center of an otherwise absorbing transition.

DOI: 10.1103/PhysRevA.94.053859

I. INTRODUCTION

There is substantial ongoing interest in quantum heat engines and refrigerators both for possible application and as part of the study of quantum thermodynamics [1]. This work began decades ago when Scovil *et al.* described the equivalence of a three level maser and a Carnot engine [2,3]. In recent years the scope of this work was significantly expanded when Scully and colleagues recognized that by using a microwave or laser source to introduce coherence and overcome "golden rule" physics that substantial improvements in performance become possible [4–6]. Work in the context of tricycle heat engines has followed and it has been recognized that the second law allows, as described in the following text, unique capabilities [7–10].

Following in this direction, this article describes the use of electromagnetically induced transparency (EIT) to construct a near-ideal but nontraditional quantum heat engine. EIT is used to establish absorptive and emissive profiles that have near zero absorption at the wavelength of maximum emission [11–15]. When this system is driven by blackbody radiation [Fig. 1(a)] because of the transparency, the radiation $B(\omega)$ in the $\pm z$ direction is much stronger than that predicted by Kirchhoff's law. This radiation has nonzero entropy, may drive a piston, and is in the category of low grade work.

Figure 1(b) shows the atomic system. The $|1\rangle \rightarrow |2\rangle$ transition is metastable with transition frequency ω_{12}. A monochromatic "coupling" laser with Rabi frequency Ω_c is applied at line center of the ω_{23} transition. Blackbody radiation at a temperature T_{13} interacts with the $|1\rangle \rightarrow |3\rangle$ transition and blackbody radiation at a temperature T_{23} interacts with the $|2\rangle \rightarrow |3\rangle$ transition. These temperatures may be different or the same, and either may be higher than the other. We assume filters on the pumping radiation that are not shown in Fig. 1. Phase matching is not involved and the directions of all of the fields are arbitrary.

In terms of the flow of input and output photons, the overall process is as follows: For each photon that is absorbed from the T_{13} reservoir a photon is generated on the T_{23} reservoir, thereby increasing the population of state $|2\rangle$ by one unit. A photon is then absorbed from the coherent coupling laser (red) on the $|2\rangle \rightarrow |3\rangle$ transition and a photon is generated on the $|3\rangle \rightarrow |1\rangle$ transition. Of note, as in nonlinear optical processes governed by the Manley-Rowe relations [16], power trades in units of photons; i.e., only a fraction ω_{23}/ω_{13} of the power generated at ω_{13} comes from the coupling laser.

II. ANALYSIS

The atomic system of Fig. 1(b) has been previously studied by Imamoğlu *et al.* [17] as a prototype closed system for lasers that do not require a population inversion. Of importance, because the system is closed, the driving blackbody excitation rates and the dephasing rates are determined by the lifetime decay rates Γ_{31} and Γ_{32} and the ambient temperatures. The rates $R_{ij} = R_{ji}$ are related to the thermal occupation numbers $\bar{n}_{13}$ and $\bar{n}_{23}$ by

$$\begin{aligned} R_{23} &= \Gamma_{32}\bar{n}_{23} = \Gamma_{32}\{\exp[\hbar\omega_{23}/k_bT_{23}] - 1\}^{-1}, \\ R_{13} &= \Gamma_{31}\bar{n}_{13} = \Gamma_{31}\{\exp[\hbar\omega_{13}/k_bT_{13}] - 1\}^{-1}. \end{aligned} \tag{1}$$

The dephasing rates of each of the transitions are

$$\begin{aligned} \gamma_{21} &= R_{23} + R_{13}, \\ \gamma_{31} &= \Gamma_{31} + \Gamma_{32} + R_{23} + 2R_{13}, \\ \gamma_{32} &= \Gamma_{31} + \Gamma_{32} + R_{13} + 2R_{23}. \end{aligned} \tag{2}$$

Therefore, once an atomic system is chosen, the only free parameters are the Rabi frequency of the coupling laser and the ambient pumping temperatures T_{13} and T_{23}. Assuming that there is no reflection or scattering into other modes, we calculate the spectral brightness $B(\omega,z)$ for a single transverse mode as a function of distance z. $B(\omega,z)$ is dimensionless so that the number of photons per second that are generated in the z direction is $1/(2\pi)\int B(\omega,z)d\omega$.

With N as the atom density, ρ_{ii} as the diagonal density matrix elements, and absorption and emission cross sections σ_{abs} and σ_{em}, the equation [18] for $B(\omega,z)$ is

$$\begin{aligned} &\frac{dB(\omega,z)}{dz} + N[\sigma_{\text{abs}}\rho_{11} - \sigma_{\text{em}}(\rho_{22} + \rho_{33})]B(\omega,z) \\ &\quad = \sigma_{\text{em}}(\rho_{22} + \rho_{33}). \end{aligned} \tag{3}$$

The spectral brightness is zero at $z = 0$ and at z sufficiently large that all spectral components of interest are absorbed reaches a maximum value of $B_{\text{black}}(\omega)$. With Λ defined as the ratio of atoms in the upper manifold to those in ground, i.e., $\Lambda = (\rho_{22} + \rho_{33})/\rho_{11}$, the limiting brightness at each spectral component is

$$B_{\text{black}}(\omega) = \frac{\Lambda\sigma_{\text{em}}}{\sigma_{\text{abs}} - \Lambda\sigma_{\text{em}}}. \tag{4}$$

*seharris@stanford.edu

2469-9926/2016/94(5)/053859(4)

We assume that field on the $|1\rangle \rightarrow |3\rangle$ transition is sufficiently weak that the populations are determined by the driving rates R_{ij} and the strong coupling field Ω_c. Solving for ρ_{ii}, Λ is

$$\Lambda = \frac{R_{13}\left[2\Omega_c^2 + \gamma_{32}(\Gamma_{32} + 2R_{23})\right]}{(\Gamma_{31} + R_{13})\left(\Omega_c^2 + \gamma_{32}R_{23}\right)}. \tag{5}$$

Following Imamoğlu *et al.*, the expressions for the absorptive and emissive cross sections are obtained by solving the density matrix equations with the assumption that the Rabi frequency of the coupling laser is large as compared to all other Rabi frequencies in the system [17,19]. With ω as the frequency of the generated spontaneous radiation and $\Delta\omega = \omega_{13} - \omega$, these cross sections are

$$\frac{\sigma_{\text{abs}}}{\sigma_0} = \frac{\gamma_{31}\left[\gamma_{21}\Omega_c^2 + \gamma_{31}\left(\gamma_{21}^2 + 4\Delta\omega^2\right)\right]}{4\Delta\omega^2\left(-2\Omega_c^2 + \gamma_{21}^2 + \gamma_{31}^2\right) + \left(\Omega_c^2 + \gamma_{21}\gamma_{31}\right)^2 + 16\Delta\omega^4}$$

$$\text{and}\quad \frac{\sigma_{\text{em}}}{\sigma_0} = \frac{\gamma_{31}\Gamma_{32}\Omega_c^2\left(\Omega_c^2 + \gamma_{21}\gamma_{31} - 4\Delta\omega^2\right) + \gamma_{31}\left[\gamma_{21}\left(\Omega_c^2 + \gamma_{21}\gamma_{31}\right) + 4\gamma_{31}\Delta\omega^2\right]\left(\Omega_c^2 + \gamma_{32}R_{23}\right)}{\left[4\Delta\omega^2\left(-2\Omega_c^2 + \gamma_{21}^2 + \gamma_{31}^2\right) + \left(\Omega_c^2 + \gamma_{21}\gamma_{31}\right)^2 + 16\Delta\omega^4\right]\left(\gamma_{32}\Gamma_{32} + 2\Omega_c^2 + 2\gamma_{32}R_{23}\right)}. \tag{6}$$

Both cross sections are normalized to $\sigma_0 = (2\omega_{13}|\mu_{13}|^2)/(\epsilon_0 c\hbar\gamma_{13})$ where μ_{13} is the transition matrix element. For a lifetime broadened transition in an isotropic medium $\sigma_0 = \lambda^2/2\pi$. The brightness is given by Eq. (4), with the population ratio and the absorptive and emissive cross sections given by Eqs. (5) and (6).

Figure 2(a) shows the cross sections for absorption and for emission, both as a function of the detuning from resonance $\Delta\omega$. In Fig. 2 (b) we assume a common pumping temperature $T_{13} = T_{23} = T_0$ and plot $B_{\text{black}}(\Delta\omega)$. As anticipated there is a narrow and strong emission at line center. [Equivalently, one may solve Eq. (3) with an optical depth of at least $N\rho_{11}\sigma_{abs}L = 10$ at all spectral components of interest to obtain nominally the same result as obtained with Eq. (4).] A point of caution: There are tails in the spectral brightness whose magnitude is determined by the optical depth that are not visible on the scale of Fig. 2(b). For example, at an optical depth at line center of 10 in the z direction, the ratio of the peak brightness $B_{\text{black}}(\Delta\omega = 0)$ to the brightness $B_{\text{black}}(\Delta\omega = \pm 10\gamma_{31})$ is 554.

Combining previous equations the brightness at line center $\Delta\omega = 0$ is

$$B_{\text{black}}(0) = -\frac{\bar{n}_{13}\left[\gamma_{21}\gamma_{32}\Gamma_{32}\bar{n}_{23} + (\gamma_{21} + \Gamma_{32})\Omega_c^2\right]}{\Gamma_{32}\bar{n}_{13}\Omega_c^2 - \gamma_{21}\left(\gamma_{32}\Gamma_{32}\bar{n}_{23} + \Omega_c^2\right)}. \tag{7}$$

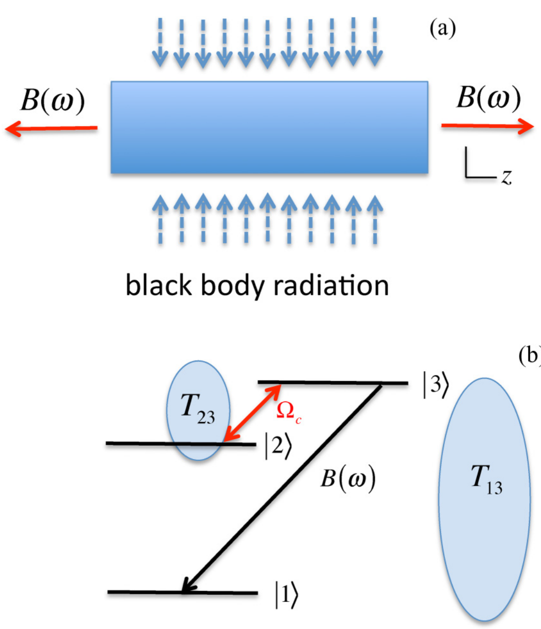

FIG. 1. (a) An ensemble of atoms is pumped by blackbody radiation. (b) The pumping temperature is T_{13} on the $|1\rangle \rightarrow |3\rangle$ transition and T_{23} on the $|2\rangle \rightarrow |3\rangle$ transition. A monochromatic "coupling" laser with Rabi frequency Ω_c is tuned to resonance of the $|2\rangle \rightarrow |3\rangle$ transition. As a result of EIT there is a spectrally narrow and bright emission in the z direction. This emission will generally have a higher temperature than that of either of the pertinent reservoirs.

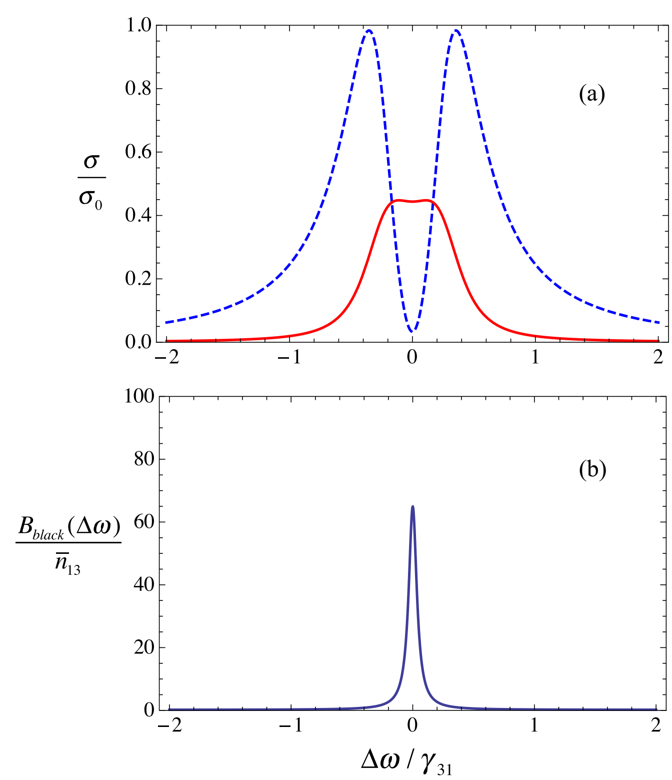

FIG. 2. (a) Absorptive (dashed line) and emissive (solid line) cross sections as a function of the detuning from resonance $\Delta\omega$. (b) Spectral brightness $B_{\text{black}}(\Delta\omega)$ normalized to the modal number $\bar{n}_{13}$. At peak the normalized brightness is 64.9 times larger than that of Kirchhoff's law. Parameters are $\Gamma_{31} = 10^7$, $\Gamma_{32} = 6 \times 10^7$, $\Omega_c = 5 \times 10^7$, $\omega_{13} = 4 \times 10^{15}$, $\omega_{12} = 10^{15}$, and $T_0 = 5778$ K. The population ratio Λ is 0.019.

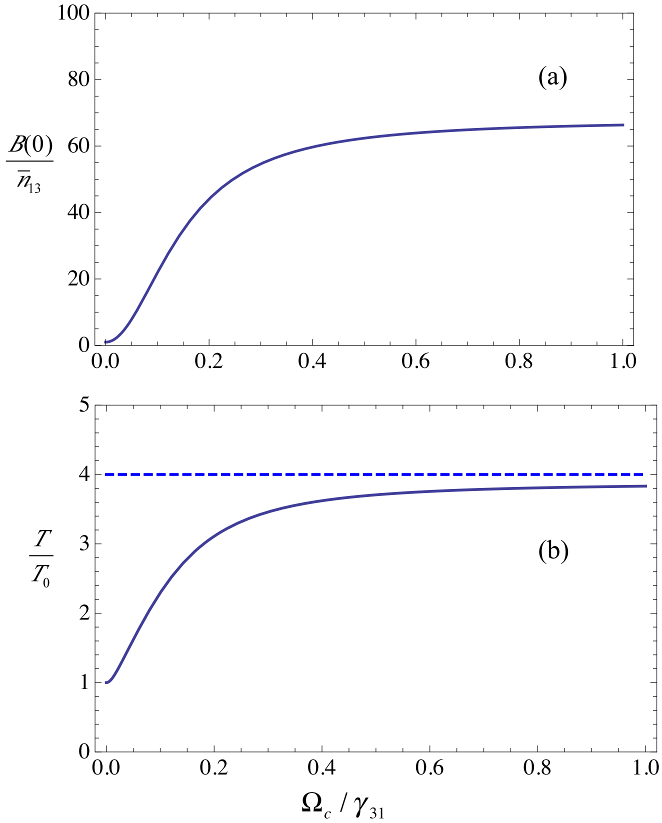

FIG. 3. (a) $B_{\text{black}}(\Delta\omega = 0)$ versus Ω/γ_{31} normalized to $\bar{n}_{13}$ and (b) the same quantity in units of normalized temperature. The parameters are the same as those of Fig. 2. The dashed line is the temperature T_B predicted by the second law.

For the atomic system of Fig. 1 there are two Feynman paths that are, independently, in detailed balance. The first is the single photon path $|1\rangle \leftrightarrow |3\rangle$. When there is no coupling laser, this is the only path and the spectral brightness $B_{\text{black}}(0) = \bar{n}_{13}$ and the equivalent temperature is T_0. The second path is the two photon path $|1\rangle \rightarrow |3\rangle \rightarrow |2\rangle$ where the transitions into and out of state $|3\rangle$ are virtual. At large Rabi frequency Ω_c this latter path is isolated and the brightness of Eq. (7) approaches

$$\lim\,[B_{\text{black}}(0), \Omega_c \rightarrow \infty] = \frac{\bar{n}_{13}[\Gamma_{31}\bar{n}_{13} + \Gamma_{32}(\bar{n}_{23}+1)]}{\Gamma_{31}\bar{n}_{13} + \Gamma_{32}(\bar{n}_{23} - \bar{n}_{13})}. \tag{8}$$

Figure 3 illustrates this behavior. Part (a) shows the line center value of the normalized brightness as a function of the Rabi frequency of the coupling laser. Part (b) shows this same quantity, but now plotted as the normalized temperature T/T_0 that is in correspondence with the spectral brightness, i.e., $T = (\hbar\omega_{13}/k)/[\ln(1/B + 1)]$.

As the strength of the coupling laser is increased the spectral brightness and equivalent temperature rise smoothly from their initial values $\bar{n}_{13}$ and T_0 to the limiting value of Eq. (8). The dashed line is the temperature as predicted by Eq. (10), and as developed in the next paragraph is greater than T_0 in the same ratio as ω_{13}/ω_{12}.

III. EIT AND THE SECOND LAW

We now compare the EIT based heat engine to an ideal engine. From Fig. 1(b): For each photon taken from the $|1\rangle \rightarrow |3\rangle$ reservoir, a photon is generated in the $|2\rangle \rightarrow |3\rangle$ reservoir. The coupling laser loses a photon to produce a photon along the z axis with a temperature T_B. Noting that the entropy of a monochromatic laser is unchanged by losing or gaining a photon [20,21], the requirement for increasing total entropy is [3,22]

$$\begin{aligned} \Delta S &= -\frac{\hbar\omega_{13}}{T_{13}} + \frac{\hbar\omega_{23}}{T_{23}} + \frac{\hbar\omega_{13}}{T_B} \geqslant 0, \\ T_B &\leqslant \frac{T_{13}T_{23}\,\omega_{13}}{T_{23}\,\omega_{13} - T_{13}\,\omega_{23}}. \end{aligned} \tag{9}$$

In Fig. 3(b), we have $T_{13} = T_{23} = T_0$, and therefore $T_B = [\omega_{13}/(\omega_{13} - \omega_{23})]T_0 = [\omega_{13}/(\omega_{12})]T_0$. The dashed line is this value. We have thereby assumed that $B_{\text{black}}(\omega)$ is in the category of low grade work and has the same entropy as a filtered thermal beam [21].

With one more approximation, $\Gamma_{31} \ll \Gamma_{32}$, Eq. (8) becomes

$$\begin{aligned} B_{\max} &= \left(\frac{\bar{n}_{23}+1}{\bar{n}_{23} - \bar{n}_{13}}\right)\bar{n}_{13}, \\ T_{\max} &= \frac{T_{13}T_{23}\,\omega_{13}}{T_{23}\,\omega_{13} - T_{13}\,\omega_{23}}, \end{aligned} \tag{10}$$

where in the last step we used $T_{\max} = (\hbar\omega_{13}/k)/[\ln(1/B_{\max} + 1)]$. Therefore, in the appropriate limits, the peak generated brightness is equal to that which is allowed by the second law. Except when close to the singularity in the denominator of Eq. (9), the approximation $\Gamma_{31} \ll \Gamma_{32}$ is not stringent. For example, in Fig. 3(b), for reasonably general parameters, the maximum value of $B(0)$ is approached. The condition that the denominator in Eq. (9) or Eq. (10) be positive sets limits on the value of the temperature of the reservoirs where the previous formulas apply. For example, if T_{13} is chosen, then T_{23} must lie in the range $(\omega_{23}/\omega_{13})T_{13} < T_{23} < \infty$.

Of importance, when $\Gamma_{32} > \Gamma_{31}$, the singularity $T_{23}\,\omega_{13} = T_{13}\omega_{23}$ or equivalently $\bar{n}_{23} = \bar{n}_{13}$ denotes the threshold for lasing without population inversion [17]. As in a normal unsaturated laser, at or above this threshold, the temperature T_B [Eq. (9)] will increase indefinitely and we may compare the efficiency of the EIT based engine to the prototype engine of Scovil and Schulz-DuBois [2] and Geusic *et al.* [3].

For normalization we first consider the energy level diagram of Fig. 1(b), but *with the coupling laser turned off*. We assume that the $|1\rangle \rightarrow |2\rangle$ transition is metastable with a small, but nonzero, matrix element. Defining the efficiency of a laser on this transition as the ratio of the per photon output energy to the input energy, the efficiency is

$$\begin{aligned} \eta_{\text{Carnot}} &= \frac{\omega_{12}}{\omega_{13}} = \frac{\omega_{13} - \omega_{23}}{\omega_{13}} \\ &= 1 - \frac{T_{23}}{T_{13}} = 1 - \frac{T_C}{T_H}. \end{aligned} \tag{11}$$

Here, the second equality follows from the population inversion condition $\omega_{23}/T_{23} = \omega_{13}/T_{13}$ and taking T_{23} as the colder of the two reservoirs.

Proceeding as above the efficiency of the EIT based engine when at threshold is

$$\eta = \frac{\omega_{13}}{\omega_{13} + \omega_{23}} = \frac{T_{13}}{T_{13} + T_{23}}. \tag{12}$$

The first equality in Eq. (12) follows by taking the input energy as the sum of the energy of a photon from the ω_{13} reservoir and a photon from the coupling laser, and the output energy as that of the generated photon at $B(\Delta\omega = 0)$. The second equality in Eq. (12) follows from the singularity in the denominator of Eq. (10), i.e., operation at reservoir temperatures that are at threshold for lasing without population inversion [23].

IV. EFFICIENCY AND SUMMARY

There are substantial differences between the efficiency of the traditional Scovil-Geusic Carnot engine and the EIT based engine. Perhaps the most important of these is that, for the EIT engine, it is not required that $T_{13} > T_{23}$, and Eq. (12) holds for both cases. When T_{13} is greater than T_{23} then, at threshold, the ratio of the efficiency of the EIT based engine generating radiation on the $|1\rangle \rightarrow |3\rangle$ transition to the Carnot engine operating on the $|1\rangle \rightarrow |2\rangle$ transition is

$$\frac{\eta}{\eta_{\text{Carnot}}} = \frac{T_{13}^2}{T_{13}^2 - T_{23}^2}. \tag{13}$$

This ratio is always greater than unity.

In summary, quantum heat engines and electromagnetically induced transparency are well known terms in quantum optics. This work has established a strong connection. We have also shown how, using the second law, one may easily obtain a result, i.e., Eq. (9), that using Maxwell's and Schrödinger's equations takes several pages of calculation, i.e., Eq. (10).

ACKNOWLEDGMENTS

A discussion of the possibility of ultrabright spontaneous emission using EIT and of the role of entropy is given in [22]. I thank Shanhui Fan for suggesting that I consider brightness enhancement in the context of heat engine physics, and thank Atac Imamoğlu, John Field, Olga Kocharovskaya, David Miller, and Marlan Scully for helpful discussions. I also thank M. Scully for showing that the change in entropy, as in Eq. (9), is exact for thermal beams.

[1] R. Kosloff and A. Levy, Quantum heat engines and refrigerators: Continuous devices, Annu. Rev. Phys. Chem. **65**, 365 (2014).

[2] H. E. D. Scovil and E. O. Schulz-DuBois, Three-Level Masers as Heat Engines, Phys. Rev. Lett. **2**, 262 (1959).

[3] J. E. Geusic, E. O. Schulz-DuBois, and H. E. D. Scovil, Quantum equivalent of the Carnot cycle, Phys. Rev. **156**, 343 (1967).

[4] M. O. Scully, Extracting Work from a Single Thermal Bath via Quantum Negentropy, Phys. Rev. Lett. **87**, 220601 (2001).

[5] M. O. Scully, M. S. Zubairy, G. S. Agarwal, and H. Walther, Extracting work from a single heat bath via vanishing quantum coherence, Science **299**, 862 (2003).

[6] M. O. Scully, Quantum Photocell: Using Quantum Coherence to Reduce Radiative Recombination and Increase Efficiency, Phys. Rev. Lett. **104**, 207701 (2010).

[7] R. Kosloff, Quantum thermodynamics: A dynamical viewpoint, Entrophy **15**, 2100 (2013).

[8] Y. Rozek and R. Kosloff, Irreversible performance of a quantum harmonic heat engine, New J. Phys. **8**, 83 (2006).

[9] M. Kolář, D. Gelbwaser-Klimovsky, R. Alicki, and G. Kurizki, Quantum Bath Refrigeration towards Absolute Zero: Challenging the Unattainability Principle, Phys. Rev. Lett. **109**, 090601 (2012).

[10] Andrei Ivanov, Yuriy Rozhdestvensky, and Evgeniy Perlin, Coherent pumping for fast laser pumping of doped crystals, J. Opt. Soc. Am. B **32**, B47 (2015).

[11] M. Fleischhauer, A. Imamoğlu, and J. P. Marangos, Electromagnetically induced transparency: Optics in coherent media, Rev. Mod. Phys. **77**, 633 (2005).

[12] O. A. Kocharovskaya and Y. I. Khanin, Coherent amplification of an ultrashort pulse in a 3-level medium without a population inversion, JETP Lett. **48**, 630 (1988).

[13] S. E. Harris, J. E. Field, and A. Imamoğlu, Nonlinear Optical Processes Using Electromagnetically Induced Transparency, Phys. Rev. Lett. **64**, 1107 (1990).

[14] S. E. Harris, Phys. Today **50**(7), 36 (1997).

[15] M. O. Scully and M. S. Zubairy, *Quantum Optics* (Cambridge University Press, Cambridge, 1997).

[16] J. M. Manley and H. E. Rowe, Some general relations of nonlinear elements 1. General energy relations, Proc. Inst. Radio Eng. **44**, 904 (1956).

[17] A. Imamoğlu, J. E. Field, and S. E. Harris, Lasers Without Inversion: A Closed Lifetime Broadened System, Phys. Rev. Lett. **66**, 1154 (1991).

[18] Diamitri Mihalas and Barbara Weibel Mihalas, *Foundations of Radiation Hydrodynamics* (Dover, New York, 1999).

[19] A. Imamoğlu, Lasers without inversion: Theory and experiment, doctorial dissertation, Stanford University, 1991.

[20] C. E. Mungan, Radiation thermodynamics with applications to lasing and fluorescent cooling, Am. J. Phys. **73**, 315 (2005).

[21] X. L. Ruan, S. C. Rand, and M. Kaviany, Entropy and efficiency in laser cooling of solids, Phys. Rev. B **75**, 214304 (2007).

[22] J. E. Field, Lasers without inversion, doctoral disseration, Stanford University, 2006.

[23] E. S. Fry, X. Li, D. Nikonov, G. G. Padmabandu, M. O. Scully, A. V. Smith, F. K. Tittel, C. Wang, S. R. Wilkinson, and S.-Y. Zhu, Atomic Coherence Effects within the Sodium D_1 Line: Lasing without Inversion via Population Trapping, Phys. Rev. Lett. **70**, 3235 (1993).